

Open-slip coupled model for simulating three dimensional bond behavior of reinforcing bar in concrete after corrosion

F. Shang & X. An

Tsinghua University, Beijing, China

T. Mishima

Maeda Corporation, Tokyo, Japan

K. Maekawa

University of Tokyo, Tokyo, Japan

ABSTRACT: Bond deterioration between reinforcing bar and concrete due to corrosion could significantly affect the residual performance of RC structures. Not only the bond model needs to be upgraded to quantify damage of interface after corrosion but also the damage state of concrete cover should be reproduced in the structural analysis. The open-slip coupled interface model that considers the effect of corrosive substance layer is first developed in this paper, which may fairly quantify the confinement state of concrete-steel interface after corrosion. Then it can be adopted for structural assessment within a new analytical approach. First, isotropic expansive strain is induced in the discrete steel bar element to simulate the expansion of corrosive substance. Afterwards, the subsequent analysis starts with the residual stress strain states of concrete solid and interface elements as input information. The experimental results can be successfully simulated. Sensitive analyses are applied to clarify the effectiveness of open-slip coupled interface model and the numerical scheme for corrosion pre-damaged RC members.

1 INTRODUCTION

Bond deterioration between reinforcing bar and concrete due to corrosion may significantly affect the residual performance of RC structures (Tachibana et al. 1990, Rodriguez et al. 1997, Coronelli et al. 2004). In the past decades, many experimental and analytical works (Al-Sulaimani et al. 1990, Auyeung et al. 2000, Coronelli 2002) have been carried out to study the concrete-steel bond characteristics after corrosion. It was found that the bond strength is slightly increased at the initial stage of corrosion owing to the pressure development at interface and finally be degraded dramatically after the splitting of concrete cover, which states the significance of confinement effect on bond.

Most of the previous works upgraded their original bond slip model of sound concrete for corroded case. Various empirical relations between reduced bond strength and corrosion loss of steel bars have been established. Whereas, much difficulty was encountered as the critical weight loss that separates the initial corrosion state and post-splitting condition of concrete cover is also governed by the confinement level. Berra et al. (2003) studied the bond deterioration after corrosion under different confinement

levels with axisymmetric FE analysis and tried to obtain the confinement effect in analysis. However, as it is logically impossible to reproduce numerical splitting crack in axisymmetric elements, specific treatment was needed to represent this effect. Thus, it will be hard to be extended to the general structure analysis. Then, the full 3D confinement effect on bond must be included in the numerical modeling.

As a matter of fact, not only interfacial area but also whole concrete cover would be damaged when steel bars are corroded. Such damage of concrete cover may influence the structural behaviors as well (Toongoenthong et al. 2005). Thus, it is of great importance to include such damage information of concrete elements in the structure analysis. Toongoenthong et al. (2005) proposed a multi-mechanical approach for the structural assessment after corrosion. The equivalent expansive strain of RC smeared element was computed according to the corrosion level and input as the initial condition for the structure analysis. The shear capacity of heavily corroded RC beams is well simulated. In this 2D approach, the greater deterioration of bond is forced to be modeled than the reality, since the web concrete and the reinforcement layer is separated in the whole

breadth of the member. Thus, the intermediate level of corrosion is hardly treated for practice.

The aim of this paper is to develop a full 3D bond model to demonstrate the confinement effect on bond after corrosion and adopt it for structure analysis with the concrete initial damage information in both interface and concrete cover.

2 OPEN-SLIP COUPLED MODEL FOR STEEL-CONCRETE BOND AFTER CORROSION

For 3D finite element analysis, the shape of reinforcing bars is idealized as cylindrical rods and the lug-concrete interaction is equivalent to an open-slip of the interface between the bars and concrete, the modeling of which is substituted in the interface element with no volume. Notably, the physical image (Fig. 1) of the interface is similar to that of the crack shear, which is governed by the open-slip of cracking surface. Then, the bond model can benefit greatly from the contact density model (Li & Maekawa 1989) for cracking shear transfer problems.

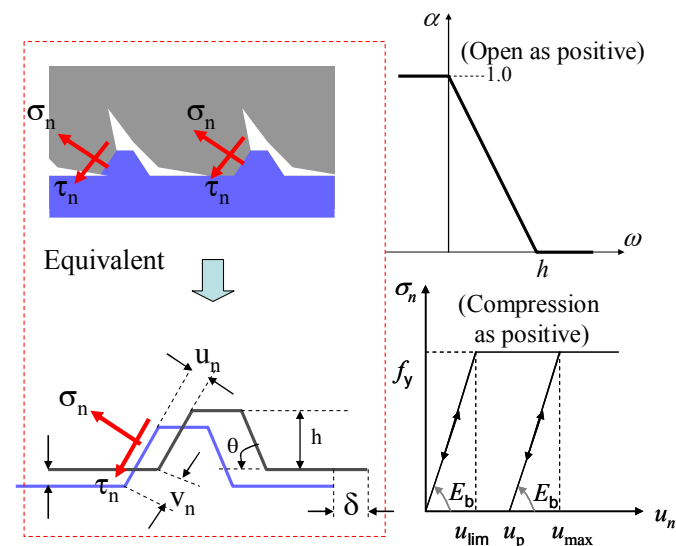


Figure 1. The open-slip coupled bond model.

It can be found that the open-slip of the interface induces normal contact and local friction between the inclined rib and surrounding concrete. Despite very accurate constitutive laws of such normal contact and local friction can hardly be obtained directly from an experiment, it is still possible to have a reasonable and simple assumption.

First, the normal contact stress σ_n^0 at the free end with zero reinforcement strain is assumed to be related only to the relative normal displacement u_n and governed by an elasto-plastic model (Fig. 1), which is expressed as follows:

$$\sigma_n^0 = f(u_n) = \begin{cases} \alpha E_b (u_n - u_p), & u_n \geq u_p \\ 0, & u_n < u_p \end{cases} \quad (1)$$

where, E_b is the stiffness of normal contact; α is the effective contact area between the inclined rib and the surrounding concrete, which is computed according to geometric relation.

$$\alpha = \begin{cases} 1, & \omega < 0 \\ 1 - \omega/h, & 0 \leq \omega \leq h \\ 0, & \omega > h \end{cases} \quad (2)$$

Here, h denotes the height of the rib. α illustrates the effect of rib height: a higher rib would result in a larger contact area with the same open interface (Fig. 1).

The variable u_p indicates the plastic component of relative normal displacement, calculated as:

$$u_p = \begin{cases} u_{\max} - u_{\lim}, & u_{\max} \geq u_{\lim} \\ 0, & u_{\max} < u_{\lim} \end{cases} \quad (3)$$

where, u_{\max} is the maximum normal displacement in the loading history and u_{\lim} is the elastic limit of relative normal displacement. Thus, the local compression yielding strength, f_y , in front of the inclined rib is calculated as:

$$f_y = E_b u_{\lim} \quad (4)$$

The bond mechanism i.e. the lug-aggregate interaction is similar to the cracking shear transfer problems, which is governed by the aggregate-aggregate interaction. Therefore, the formulation of contact stiffness E_b^0 and local yielding strength f_y of sound steel-concrete bond can refer to the research on the cracking shear transfer (Maekawa et al. 2003), which is expressed as follows:

$$\begin{cases} E_b^0 = 343 f_c'^{(1/3)} \text{ (MPa/mm)} \\ f_y = 13.7 f_c'^{(1/3)} \text{ (MPa/mm)} \end{cases} \quad (5)$$

The effect of corrosive substance layer between sound steel and concrete has to be taken into account after corrosion of steel bar. As shown in Figure 2, we have the total equivalent contact spring as:

$$\frac{1}{E_b} = \frac{1}{E_b^0} + \frac{\eta}{G_{\text{cor}}} \quad (6)$$

Here, G_{cor} is the stiffness of corrosive substance (around 7GPa: Toongonthong et al. 2005), and η is corrosive substance depth and can be computed as:

$$\eta = \left(\sqrt{1 + \alpha\gamma} - 1 \right) \cdot d/2 \quad (7)$$

where, γ denotes the mass fraction loss and α is the coefficient of expansion of corrosive substance, which ranges from 2~6 depending on the composition of oxides according to the previous literature (Liu et al. 1998).

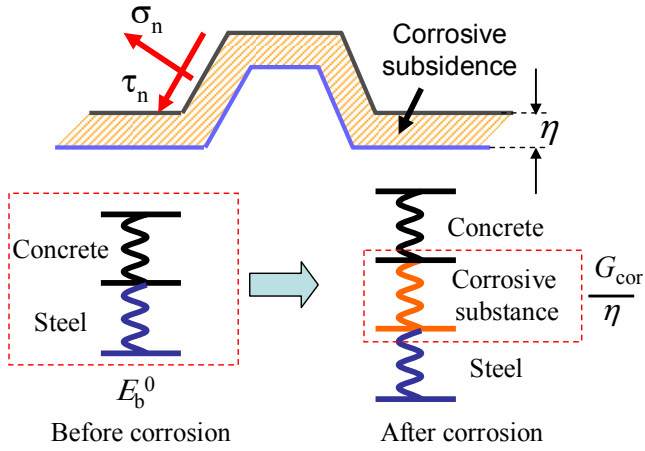


Figure 2. Concrete-steel interface model after corrosion.

As reported by Shima et al. (1987), the reinforcement strain can be used to describe the effect of micro-defect of cover concrete on the local bond. Here, the reinforcement strain represents the damaged state of surrounding concrete, i.e. the width of Goto crack, which is almost parallel to the normal contact stress (Maekawa et al. 2003). The concrete compression performance parallel to the crack decreases as the transverse crack width increases (Collins & Vecchio 1982). The increase in reinforcement strain, i.e., the increase of Goto crack width, will certainly reduce the normal contact stress as well, which stands for the compressive behavior of such a micro-cracked concrete strut in front of a rib, too. Thus, the normal contact stress at an arbitrary location is expressed as:

$$\sigma_n = \frac{\sigma_n^0}{1 + \varepsilon \times 10^\lambda} \quad (8)$$

where, ε is the axis tensile strain of the corresponding reinforcing bar element. And $\lambda=3.5$ based on the sensitivity analysis.

As shown in Figure 3, the Mohr-Coulomb's friction along the inclined rib τ_n (compression side) is formulated as follows:

$$\begin{cases} d\tau_n = \alpha G_n dv_n \\ \int_{path} d\tau_n \leq \mu \sigma_n \end{cases} \quad (9)$$

where, G_n is the tangential stiffness along the inclined rib, and v_n is the relative normal and tangential displacements. The Poisson effect of the interface is denied here. Then, we have:

$$G_n = 0.5E_n \quad (10)$$

According to the experiments by Xu et al. (1994), μ is around 0.2~0.3 (in this paper, $\mu=0.25$).

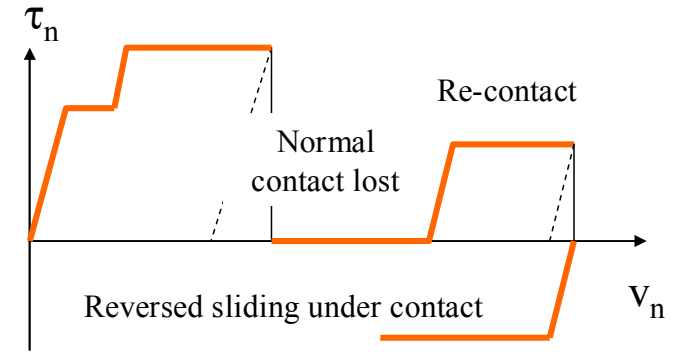


Figure 3. Constitutive law for Mohr-Coulomb's friction along inclined rib.

All together, 3D bond stress field can be computationally summarized as:

$$\begin{cases} \tau_b = \frac{1}{L} (\sigma_n \sin \theta + \tau_n \cos \theta) \\ \tau_\varphi = E_\varphi \delta_\varphi \\ \sigma = \frac{1}{L} (-\sigma_n \cos \theta + \tau_n \sin \theta) \end{cases} \quad (11)$$

where, τ_b is defined as bond stress, σ is the dilatant stress, L denotes the spacing of ribs in a longitudinal direction; τ_φ , E_φ and δ_φ are the shear stress, stiffness and shear slip along the hoop direction of the reinforcement. By considering that the torsion of the reinforcing bars seldom occurs in the structure, the authors assume the linear elasticity in the hoop direction of reinforcement with relatively large stiffness.

The relative displacement in both normal and tangential directions along the inclined rib (compression side) can be computed from the local open and local slip of the interface as:

$$\begin{bmatrix} u_n \\ v_n \end{bmatrix} = \begin{bmatrix} s & -c \\ c & s \end{bmatrix} \begin{bmatrix} \delta \\ \omega \end{bmatrix} \quad (12)$$

where, $s=\sin\theta$, $c=\cos\theta$. θ is the inclined angle of the rib, ω and δ are the local opening and local slip of the interface, respectively.

3 SIMULATION OF BOND AFTER CORROSION

3.1 Analytical scheme

A computational scheme is proposed here to simulate the residual bond after corrosion. The splitting

of concrete cover due to expansion of corrosive substance is first simulated by imposing isotropic forced volumetric strain on the reinforcement elements. Orthotropic expansion is to induce the radial deformation without any elongation of reinforcement elements. So, the tensile stress is resultant in the circumferential direction in concrete, which leads to splitting cracks. Analysis of this stage is defined as corrosion pre-damage one and it is terminated when the splitting crack width reaches the reality.

Second, the subsequent analysis is followed for the structural assessment. Here, the residual stress and strain states of concrete solids and interface elements, which was produced by the first stage of analysis, is the input data for the starting states. The effect of damaged concrete cover and confinement on bond can be consistently taken into account in the simulation. Analysis of this stage is defined as the re-start stage.

3.2 Corroded RC beam

Some of the corroded RC beams without any web reinforcement tested by Tachibana et al. (1990) were used. Figure 4 shows the specimen details and reinforcement arrangement. The concrete strength is 35.6 MPa and the yield strength of reinforcement is 353 MPa with a tensile reinforcement ratio of 1.3%. The shear span to depth ratio is 4.2.

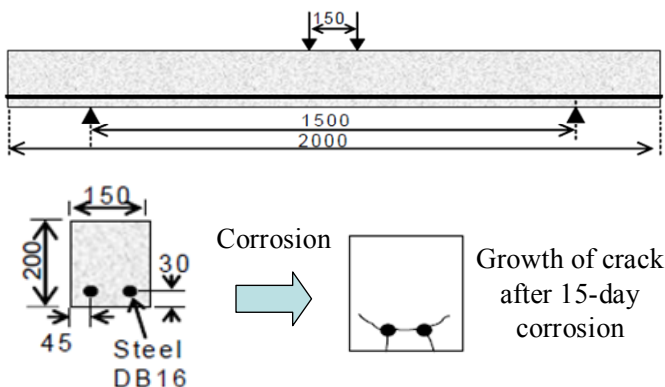


Figure 4. Corroded beam tested by Tachibana et al. (1990).

Table 1a. Parameters of reinforcement geometry for analysis.

Diameter	θ	h	L
Mm	°	mm	mm
16	45	1.0	10.0

Table 1b. Parameters of open-slip coupled model for each case in analysis.

Bottom crack width	η	E_b	f_y
Mm	mm	GPa/mm	MPa
0.0 (Non-damage)	0.00	11.2	45.0
0.10	0.36	10.3	45.0
0.40	0.59	9.9	45.0
0.75	1.07	9.2	45.0
1.50	1.89	8.4	45.0

These beams were subjected to galvanostatic-corrosion at first and then statically loaded to failure. The corrosion cracks opened widely in the bottom surface and propagated to the side surface. The effect of different corrosion levels (bottom crack width=0.0mm~0.75mm) were studied in the experiment. It was found that the failure pattern gradually changed from flexure to the bond-shear one.

3D-quadrilateral solid elements were applied in the finite element analysis for both reinforcing bars and the surrounding concrete. The interface element with no volume was used between the reinforcement and concrete, governed by the opening-slip coupled interface model. All the parameters used for open-slip coupled model are listed in Table-1a and 1b.

The reinforcement was simulated as the elastoplastic hardening material. The surrounding concrete is modeled by the 3D multi-directional smeared crack approach so that the interaction between corrosive cracks and local bond cracks can be simulated. Here, the authors skip the details of the constitutive models, which have been verified in the past research and can be refer to Maekawa et al. (2003).

4 NUMERICAL SIMULATION

4.1 Simulation of corrosive substance expansion

In the corrosion pre-damage analysis, smeared splitting cracks were produced in the concrete cover elements. Figure 5 shows the 1st principle strain distribution for the different corrosion level. The numerical crack appeared in the bottom surface first, and then to the side surface, which could be verified by the experimental observations as shown in Figure 4.

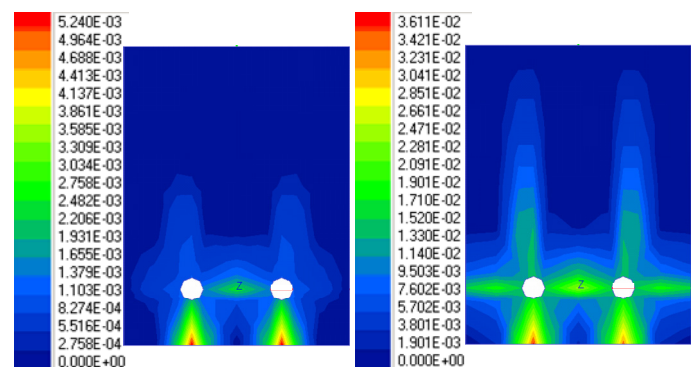


Figure 5. 1st Principle strain distribution in the cross section after corrosive substance expansion.

In addition, residual stress and relative displacement were also produced in the interface element, as shown in Figures 6a and 6b. It could be found that no slip and bond stress exist. Whereas, stress and relative open displacement were made in the dilatant direction, which describes the pressure development due to the corrosive substance expansion. When the

splitting crack grew wider and wider, the dilatant stress would dramatically decreased and interface displacement changes from closure to open, which hints the loss of contact between lug of the steel and concrete in corrosion, and much weaker bond performance was expected in the next stage of analysis. Thus, the confinement effect on bond would effectively be illustrated.

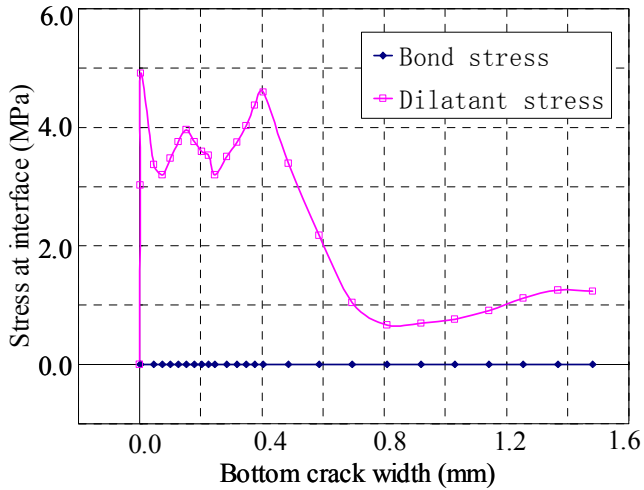


Figure 6a. Residual stress state at the interface after corrosive substance expansion.

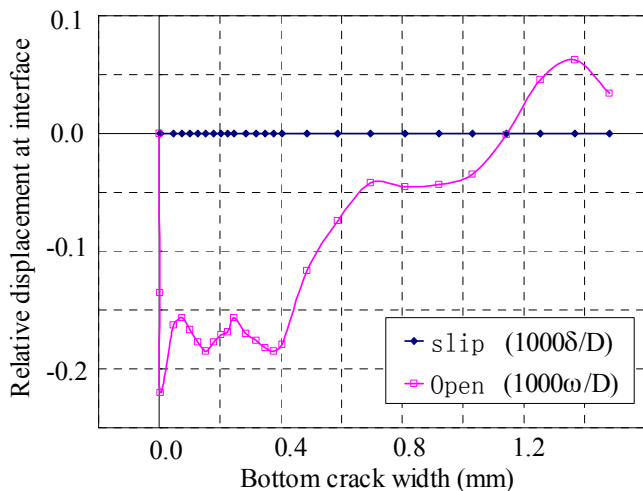


Figure 6b. Residual relative displacement at interface after corrosive substance expansion.

4.2 Simulation of mechanical loading tests after corrosion

The re-start stage of analyses were carried out with the above residual stress strain information recorded as the initial conditions. Figure 7 shows the computed capacity of each corroded case compared with the experiment data and results of Toongoenthong et al.'s 2D simplified approach (2005). More realistic capacity is obtained. Not only the reduction of capacity due to corrosion is reproduced but the slightly increase at initial corrosion stage as well. The 2D simplified approach gives the lower capacity as explained in Chapter 1 and leads to over-safety estimation for practice, since the corrosion crack is inevita-

bly modeled to penetrate over the whole breadth of the RC member.

The failure pattern is computationally changed from flexure to bond-shear failure as shown in Figure 8a and Figure 8b. In these cases, the beam capacity may strongly rely on the anchorage of main reinforcement. Then, the corroded bond state must be quantitatively evaluated in the structural assessment in more details.

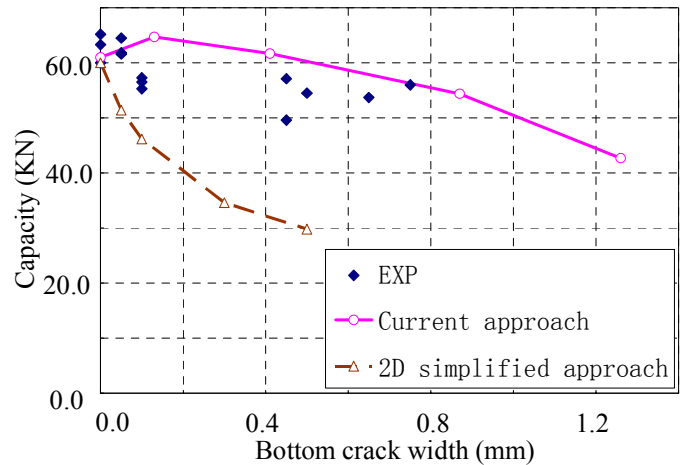


Figure 7. Experimental and analytical capacity of corroded beam (2D simplified approach: Toongoenthong et al. 2005).

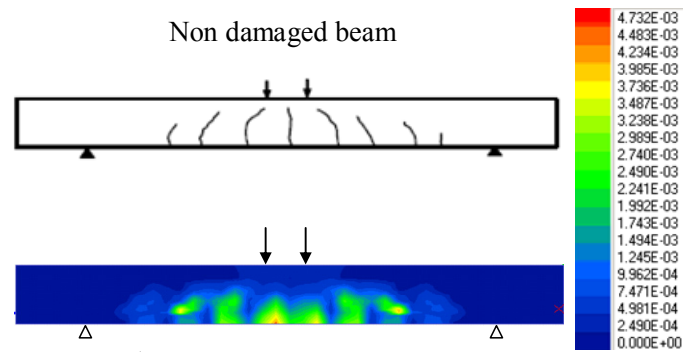


Figure 8a. 1st Principle strain distribution of non damaged beam at failure.

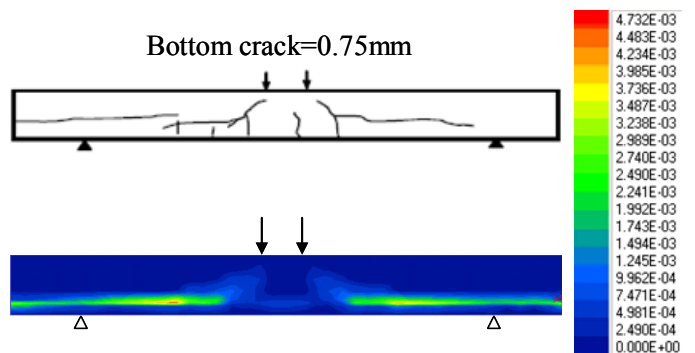


Figure 8b. 1st Principle strain distribution of corroded beam (bottom crack=0.75mm) at failure.

4.3 Effectiveness of the open-slip coupled model and corrosion damage initialization

Sensitive analyses of the above case with 0.75mm width crack at bottom surface were carried out to clarify the effectiveness of open-slip coupled inter-

face model and the analytical approach for corrosion pre-damage analysis. The case without interface element and the case without corrosion pre-damage analysis were studied respectively as lined-up in Table-2.

Figure 9 shows the computed load-displacement relation of each case compared with the experiment data. It is noted that the anchorage failure could not be reproduced when only the 2nd stage of analysis was applied for analysis, while it would underestimate the capacity of the corroded beam when the open-slip bond model is not used.

It implies that both the residual damage states at interface and concrete cover produced by corrosion have significance on the structural assessment of the beam capacity. The splitting of concrete cover at anchorage zone could not only affect the residual bond strength, but leads to shear failure as well when such crack connects to the diagonal crack. Hence, it is of great necessity to take it into account in the analysis.

On the other hand, during the corrosion pre-damage analysis, the concrete-steel contact will be gradually lost as the increase of corrosion level as discussed above. The bond stress transfer mechanism would be dramatically changed at this stage. However, it has been reported both in experiment and analysis that the shear capacity of the beam without web reinforcement increases when the bond of main reinforcement in shear span is completely eliminated (Soltani 2002, Wang 2007). Thus, case C which denied the open-slip model by sharing the nodes between steel and concrete elements in the analysis would certainly produce too much bond stress and result in less capacity.

Table 2. Sensitive cases for 0.75mm width of bottom crack.

	Open-slip model.	Corrosion damage analysis
Case A	used	used
Case B	used	not used
Case C	not used	used

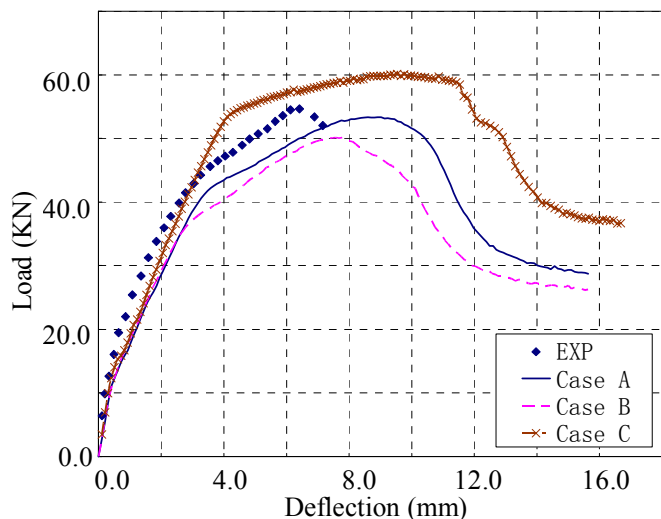


Figure 9. Sensitive analyses for case with 0.75mm width of bottom crack.

5 CONCLUSIONS

Not only the damage of interface but also the damage of the concrete cover produced by the corrosive substance expansion has to be quantitatively considered in the structural assessment. The open-slip coupled model is developed to quantify the confinement effect on bond and successfully applied for structural analyses within corrosion pre-damage analysis. Compared with the 2D analytical approach, the accuracy of the behavioral simulation is upgraded since the transient process of corrosive cracks can be simulated in the full 3D extent. And the effectiveness of both open-slip model and corrosion pre-damage analysis is clarified.

REFERENCES

- Al-Sulaimani, G. J., Kaleemullah, M. and Basumbul, I.A. 1990. Influence of corrosion and cracking on bond behavior and strength of reinforced concrete members. *ACI Structure Journal*: Vol.87, No.2, Mar.-Apr. pp.230-231.
- Auyeung, Y.B., balaguru, P. and Chung, L. 2000. Bond behavior of corroded reinforcement bars. *ACI Material Journal*: 97(2),214-220.
- Berra, M., Castellani, A., Coronelli, D. Zanni, S. and Zhang, G. 2003. Steel-concrete bond deterioration due to corrosion: finite-element analysis for different confinement levels. *Magazine of Concrete Research*: 2003, 55, No.3, June, 237-247.
- Collins, M.P. and Vecchio, F. 1982. The response of reinforced concrete to in-plane shear and normal stresses, *University of Toronto*, 1982
- Coronelli, D. 2002 Corrosion cracking and bond strength modeling for corroded bars in reinforced concrete. *ACI Structure Journal*: 99(3),267-276.
- Coronelli, D., and Gambarova, P. 2004 Structural Assessment of Corroded Reinforced Concrete Beams: Modeling Guidelines. *Journal of Structural Engineering*: ASCE, 130(8), 1214-1224.
- Li, B. Maekawa, K. and Okamura, H. 1989. Contact density model for stress transfer across crack in concrete. *J. Faculty Eng, University of Tokyo (B)*: Vol. 40, No. 1, pp. 9- 52.
- Liu, Y. and Weyers, R.E. 1998. Modeling the Time-to-Corrosion Cracking in Chloride Contaminated Reinforced Concrete Structures. *ACI Materials Journal*: V.95, No.6. Nov.-Dec. 1998
- Maekawa, K., Pimanmas, A. and Okamura, H. 2003. Nonlinear Mechanics of Reinforced Concrete. *Spon Press*, London.
- Rodriguez, J., Ortega, L.M., and Casal, J. 1997. Load carrying capacity of concrete structures with corroded reinforcement. *Construction and Building Materials*: Vol, 11, No.4, pp. 239-248, 1997
- Shima, H., Chou, L., and Okamura, H. 1987. Micro and macro models for bond in reinforced concrete. *J. Fac. Eng., Univ. Tokyo (B)*, 39(2), 133- 194.
- Soltani, M., 2002. Micro Computational Approach to Post-cracking Constitutive Laws of Reinforced Concrete and Application to Nonlinear Finite Element Analysis. (Doctor thesis). *University of Tokyo*.
- Tachibana, Y., Kajikawa, Y., and Kawamura, M. 1990 The mechanical behavior of RC beams damaged by corrosion of reinforcement. *Concrete Library of JSCE*: 14, March, 177-188.

- Toongoenthong, K. and Maekawa, K. 2005. Multi-Mechanical Approach to Structural Performance Assessment of Corroded RC Members in Shear. *Journal of Advanced Concrete Technology*, 3(1),107-122.
- Xu et al. Y., Shen W and Wang H. 1994. An experimental study of bond-anchorage properties of bars in concrete. (in Chinese) *Journal of Building Structures*: 15(3), 27– 36
- Wang, C. 2007. Application of Simplified Embedded Model in The Analysis of Nonlinear Mechanics of RC structures (Master thesis in Chinese). *Tsinghua University*.